Brief Communication

Visualization of plasticity in fear-evoked calcium signals in midbrain dopamine neurons

Bryan B. Gore,[1,2,3] Marta E. Soden,[1,2,3] and Larry S. Zweifel[1,2]

[1]Department of Pharmacology and [2]Department of Psychiatry and Behavioral Sciences, University of Washington, Seattle, Washington 98053, USA

Dopamine is broadly implicated in fear-related processes, yet we know very little about signaling dynamics in these neurons during active fear conditioning. We describe the direct imaging of calcium signals of dopamine neurons during Pavlovian fear conditioning using fiber-optic confocal microscopy coupled with the genetically encoded calcium indicator GCaMP3. We observed calcium transients in a subset of dopamine neurons to an unconditioned fear stimulus on the first day of Pavlovian fear conditioning. On the second day, calcium transients occurred in response to conditioned and unconditioned stimuli. These results demonstrate plasticity in dopamine neuron calcium signals and the occurrence of activity-dependent processes in these neurons during fear conditioning.

[Supplemental material is available for this article.]

Discovering the nature of behaviorally evoked calcium signals within discrete neural populations in the brain is critical for elucidating the role of calcium in neural circuit regulation. Recent advances in the development of fluorescent genetically encoded calcium indicators have made it possible to monitor calcium dynamics at the single-cell and single-synapse levels (Tian et al. 2012). When coupled to two-photon microscopy, gradient index lenses, fiber-optics, or miniaturized microscopes, genetically encoded indicators allow unprecedented access to select neural populations to define calcium dynamics in behaving animals (Kerr and Nimmerjahn 2012).

Dopamine neurons of the ventral tegmental area (VTA) convey essential signals for salience detection, motivation, and reward processes (Bromberg-Martin et al. 2010; Schultz 2013). Pharmacological and genetics studies have broadly implicated dopamine in fear-related learning (Pezze and Feldon 2004), yet the extent to which dopamine neurons are activated during fear processing remains uncertain (Lammel et al. 2013; Schultz 2013). Studies measuring putative dopamine neuron responses to aversive stimuli have yielded far ranging results, from activating only a small percentage of cells (Mirenowicz and Schultz 1996) to activating a third or more of the total dopamine neuron population (Chiodo et al. 1979; Mantz et al. 1989). Similar disparities have been reported for midbrain neuron responses to conditioned stimuli previously paired with an aversive event (Guarraci and Kapp 1999; Joshua et al. 2008; Matsumoto and Hikosaka 2009). Major contributors to these disparate results are imperfect methods used to identify dopamine neurons in vivo (Ungless and Grace 2012).

Considerable extrapolations have been made regarding the connection between dopamine neurons and fear processes based on the electrophysiological responses to aversive stimuli (Pezze and Feldon 2004; Lammel et al. 2013; Schultz 2013); however, few studies have directly determined whether the neurons recorded were dopamine-producing cells (Ungless et al. 2004; Brischoux et al. 2009). Activation of midbrain neurons to fear-conditioned stimuli have also been reported (Guarraci and Kapp 1999), but again, it is unknown whether these are dopamine neurons. Dopamine neurons undergo plasticity following noxious stimulus presentation (Lammel et al. 2011), yet whether these changes are similarly associated with fear-inducing stimuli is not clear. Visualization of calcium dynamics in genetically defined dopamine neurons of the freely moving mouse allows for a direct assessment of activity-dependent processes during fear conditioning.

Fiber-optic confocal (FOC) fluorescence microscopy provides the capability to access deep structures in the brain. Consisting of a small diameter (<350 μm) array of 1 μm fiber optics coupled to a micro-objective (Laemmel et al. 2004), laser scanning across the fiber bundle provides sufficient resolution to detect fluorescence at the single-cell level (Vincent et al. 2006). Here we used FOC fluorescence microscopy to visualize activity-dependent calcium signals in genetically isolated dopamine neurons in freely moving mice. Following Pavlovian fear conditioning, we observed plasticity in calcium signals, whereby neurons with calcium transients to the conditioned stimulus (CS) emerged following conditioning.

To selectively detect calcium signals in dopamine neurons of the VTA, we generated a conditional adeno-associated viral vector (AAV) containing double-inverted lox (DIO or FLEX) sites flanking the inverted open-reading frame of GCaMP3 (Tian et al. 2009) (AAV-FLEX-GCaMP3) (Fig. 1A). Injection of AAV-FLEX-GCaMP3 into the VTA of mice expressing Cre recombinase under the control of the endogenous dopamine transporter locus (*Slc6a3*$^{Cre/+}$) (Zhuang et al. 2005) led to selective expression in dopamine neurons (Fig. 1B,C; percent GCaMP3-positive neurons that co-expressed TH: $99.21 \pm 0.223\%$, $n = 5$ mice). To ensure GCaMP3 expression does not alter dopamine neuron physiology, we monitored spontaneous action potentials in acute brain slices; no discernible differences in action potential waveform or firing frequency were detected between transduced and non-transduced neurons (Fig. 1D–F).

[3]These authors contributed equally to this work.
Corresponding author: larryz@u.washington.edu
Article is online at http://www.learnmem.org/cgi/doi/10.1101/lm.036079.114.

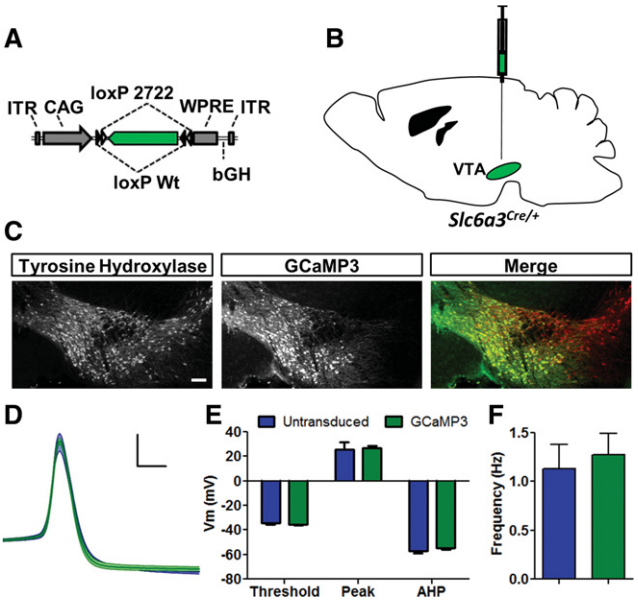

Figure 1. Expression of GCaMP3 in dopamine neurons. (*A*) Schematic of AAV-FLEX-GCaMP3. (*B*) Schematic of viral injection to the midbrain. (*C*) Immunohistochemistry illustrating GCaMP3 colocalization with the dopamine neuron marker tyrosine hydroxylase (TH). Scale = 100 μm. Note: GCaMP3 expression is largely restricted to the medial aspect (VTA) of the ventral midbrain. (*D*) Average action potential waveforms for VTA neurons transduced (green) or untransduced (blue) with AAV-FLEX-GCaMP3 (scale, 2 msec, 20 mV). (*E*) Average waveform properties of untransduced ($n = 6$) and transduced ($n = 7$) cells in *D*. (*F*) The average firing rate of transduced and untransduced neurons in the VTA. Data are presented as mean ± SEM.

To determine whether changes in GCaMP3 fluorescence could be observed by FOC fluorescence microscopy, we used an acute brain slice preparation. When the fiber optic was directly lowered onto the slice, we could easily detect fluorescence from GCaMP3 (Fig. 2A–C). Next, we monitored whether intrinsic activity in the slice influences GCaMP3 fluorescence by bath applying the $GABA_A$ receptor agonist muscimol (10 μM; 3.5 min). GABA-mediated inhibition led to a small but detectable reduction in GCaMP3 fluorescence (Fig. 2D). To determine the upper limits of calcium detection, we stimulated direct calcium influx through activation of NMDA-type glutamate receptors by bath application of NMDA (20 μM; 3.5 min). NMDA evoked a robust increase in fluorescence signal (Fig. 2D). These results demonstrate that GCaMP3 fluorescence is reliably detected using FOC microscopy, albeit less robustly than with conventional wide-field (WF) fluorescence microscopy (two-way repeated-measures ANOVA, $F_{(117,2691)} = 14.51$, $P < 0.0001$; Fig. 1G).

Salient behavioral stimuli have been demonstrated to transiently increase spike firing in dopamine neurons (Bromberg-Martin et al. 2010), and GCaMP3 has been shown to increase fluorescence reliably to brief action potential trains (Tian et al. 2009). To determine whether GCaMP3 could detect calcium signals in dopamine neurons in response to different action potential trains, we used either WF or FOC microscopy to monitor GCaMP3 fluorescence in response to action potentials generated at varying frequencies and durations by an extracellular stimulating electrode placed rostral to the VTA. Action potential generation was confirmed using whole-cell patch clamp with simultaneous WF imaging of GCaMP3 fluorescence (Fig. 2E,F). Subsequently, the patch electrode was removed, the fiber-optic probe was lowered onto the slice, and calcium signals were imaged using the same stimulation parameters. Both WF and FOC microscopy detected fluorescence signal changes during trains of 10 spikes at 20 Hz, 5 spikes at 20 Hz, and a 5 spike-simulated burst epoch (Fig. 2G). Fluorescence signals detected with fiber-optic microscopy had a similar time course to signals detected with WF microscopy (Fig. 2H,I), but generally had a smaller peak amplitude (Fig. 2J), although this did not reach statistical significance.

Based on our ability to detect activity-dependent calcium transients ex vivo, we tested whether calcium signals could be detected in freely behaving mice during fear conditioning. AAV-FLEX-GCaMP3 was injected into the VTA of *Slc6a3*$^{Cre/+}$ mice through a specialized cannula attached to the skull over the midbrain (Fig. 3A,B). On the day of conditioning, the fiber optic was lowered through the cannula until fluorescence signal from

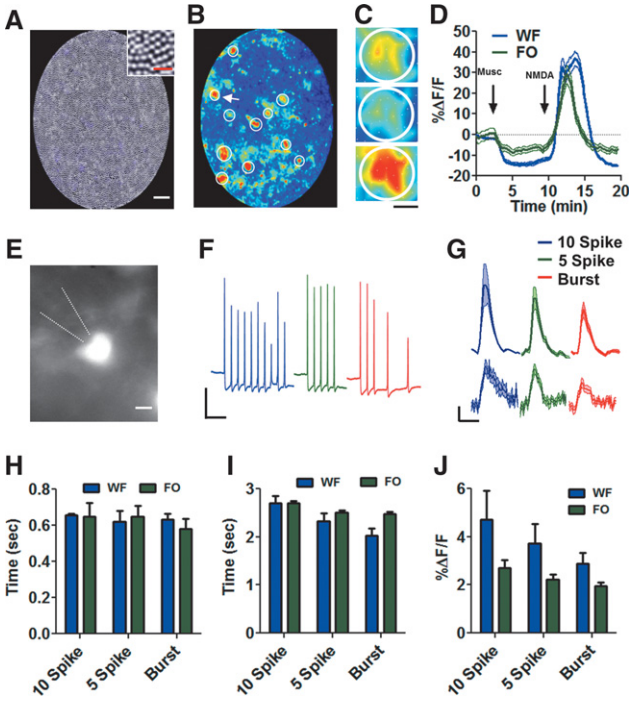

Figure 2. Characterization of activity-dependent GCaMP3 fluorescence in brain slice. (*A*) Illustration of individual fiber bundles comprising the field of view (scale 40 μm). (*Inset*) Higher magnification demonstrating individual fiber-optic arrangements within the probe (scale 10 μm). Characterization as a single cell requires detection by a minimum of four fibers, or an average diameter of 6 μm. (*B*) Jet pseudocolor fiber-optic image of dopamine neurons in an acute slice following NMDA application. White circles highlight individual cells. (*C*) High magnification view of cell in (*B*) indicated by arrow during baseline (*top*), muscimol (*middle*), and NMDA (*bottom*). White dots illustrate the center of individual fibers and circles represent ROI used for analysis (scale = 10 μm). (*D*) The change in fluorescence observed following bath application of muscimol and NMDA (blue, WF = wide-field, $n = 7$; green FO = fiber optic, $n = 19$). Arrows indicate the time of application. Data are presented as mean ± SEM. (*E*) WF fluorescence image of GCaMP3 expressing dopamine neuron illustrating patch electrode placement (dashed lines) to record action potential generation during imaging (scale 10 μm). (*F*) Average traces of stimulated action potentials recorded during imaging (three trials). Scale = 20 mV, 250 msec. (*G*) Change in GCaMP3 fluorescence observed following action potential stimulation using WF (*top*, $n = 7$ for 10 spikes and $n = 19$ for both 5 spikes and burst) or FO microscopy (*bottom*, $n = 34$ for 10 spikes, and $n = 28$ for both 5 spikes and burst). Scale = 1%DF/F, 2 sec. (*H*) Average latency to onset of fluorescence intensity change following action potential stimulation measured using FO or WF fluorescence microscopy. (*I*) Average duration of fluorescence change following action potential stimulation. (*J*) Average peak fluorescence intensity change. Data are presented as mean ± SEM.

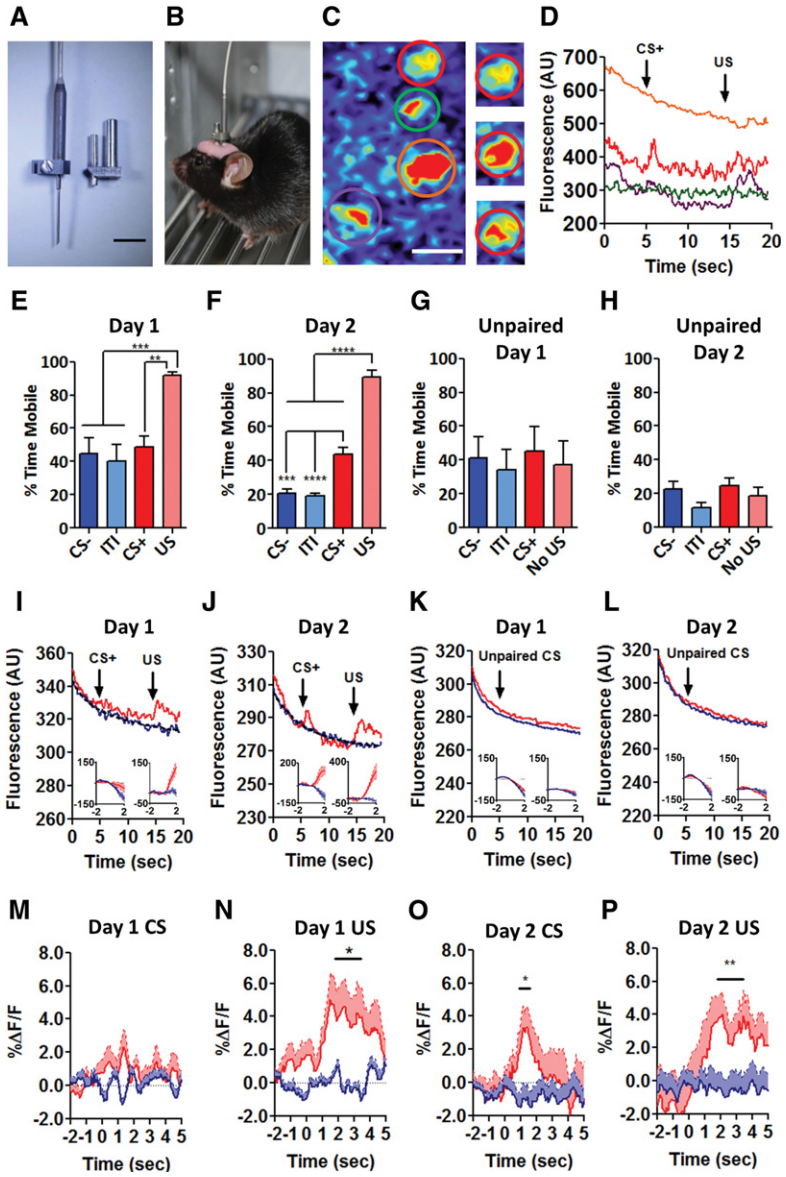

Figure 3. Characterization of calcium signals in dopamine neurons during fear conditioning. (*A*) Image of fiber-optic probe (*left*) and cannula (*right*). Scale (5 mm). (*B*) Image of mouse in conditioning chamber showing fiber-optic/cannula assembly. (*C*) Image of GCaMP3 fluorescence in VTA obtained by the fiber optic in vivo on second day of fear conditioning (scale 20 μm), (*left*) four cells (colored circles correspond to graph in (*D*); (*right*) fluorescence of a single cell during baseline (*top*), immediately after CS+ (*middle*), and immediately after shock (*bottom*). (*D*) Fluorescence signal acquired from four cells in (*C*) during a single trial on the second day of conditioning; red line is the cell in the *right* panels in (*C*). (*E*) Percent time mobile on Day 1 of paired trials (Bonferroni post hoc [**] $P < 0.01$, [***] $P < 0.001$). (*F*) Percent time mobile on Day 2 of paired trials. (Bonferroni post hoc [***] $P < 0.001$, [****] $P < 0.0001$.) (*G*) Percent time mobile on Day 1 of unpaired trials. (*H*) Percent time mobile on Day 2 of unpaired trials. (*I*) Average change in fluorescence observed during Day 1 of conditioning in CS+ (red) and CS− (blue) trials. *Insets* are average CuSums of cells responding to the US during CS presentation (*left*, red CS+ trials, blue CS− trials) or US presentation (*right*, red CS+ trials, blue CS− trials); *x*-axis: time (sec), 2 sec prior and 2 sec following stimulus; *y*-axis: cumulative summation of fluorescence signal. (*J*) Average change in fluorescence observed during Day 2 of conditioning in CS+ (red) and CS− (blue) trials. *Insets* are average CuSums of cells responding to the US during CS presentation (*left*, red CS+ trials, blue CS− trials) or US presentation (*right*, red CS+ trials, blue CS− trials). (*K*) Average change in fluorescence observed during Day 1 of conditioning with unpaired CS+ (red) and CS− (blue). *Insets* are average CuSums of all cells. (*L*) Average change in fluorescence observed during Day 2 of conditioning with unpaired CS+ (red) and CS− (blue). *Insets* are average CuSums of all cells. (*M*) Average normalized percent change in fluorescence during CS+ (red) and CS− (blue) trials on Day 1. (*N*) Average normalized percent change in fluorescence during US (red), or corresponding time in CS− (blue) trials on Day 1 (Bonferroni post hoc [*] $P < 0.05$; time: 0.833–2.417 sec). (*O*) Average normalized percent change in fluorescence during CS+ (red) and CS− (blue) trials on Day 2 (Bonferroni post hoc [*] $P < 0.05$; time: 1.083–1.833 sec). (*P*) Average normalized percent change in fluorescence during US (red), or corresponding time in CS− (blue) trials on Day 2 (Bonferroni post hoc [**] $P < 0.01$; time: 1.417–3.833 sec).

dopamine neurons was detected (Fig. 3C). The probe was then stabilized by direct attachment to the cannula and dopamine neurons were imaged during a Pavlovian fear conditioning paradigm. Mice were conditioned for 10 trials to a CS (CS+, 10 sec continuous chamber illumination) that coterminated with a US (0.5-sec–0.3-mA foot shock). Interleaved with CS/US pairings was the delivery of 10 CS− trials (10 sec of flashing LED lights). Cells were imaged for a total of 20 sec for each trial (5 sec before CS onset and 5 sec following US termination) (Fig. 3D). An additional cohort of mice was imaged during cue presentations without receiving foot shock (unpaired).

To determine whether mice tethered to the fiber-optic probe moved freely during conditioning, we monitored mobility by video tracking. To isolate mobility unrelated to foot shock during CS+ presentations, we analyzed the animal's activity during the first 9.5 sec of the CS+, excluding the 0.5 sec of foot shock. In addition, we analyzed mobility during times corresponding to the first 9.5 sec of CS− presentation, 9.5 sec of the intertrial interval (ITI) period following CS− presentation, and 9.5 sec of US presentation that included 0.5 sec of shock and 9 sec of ITI following shock termination. During the first day of imaging in both paired and unpaired trials, mice were mobile (grooming, locomoting, or making orienting head movements) ~40% of the time during all periods, except during the period of US presentation in which the mice displayed significantly increased activity in response to the foot shock (Fig. 3E,G; two-way repeated-measures ANOVA, $F_{(3,28)} = 9.878$, US vs. CS− or ITI, $P < 0.001$, US vs. CS+, $P < 0.01$, $n = 8$ mice). On the second day of conditioning, mice were relatively immobile in both paired and unpaired conditions; however, mobility was significantly increased during CS+ and US presentations in the paired trials (Fig. 3F,H; two-way repeated-measures ANOVA, $F_{(3,28)} = 97.90$, US vs. CS−, ITI, or CS+, $P < 0.0001$, CS− vs. CS+, $P < 0.001$, CS+ vs. ITI, $P < 0.0001$, $n = 8$).

To determine whether fluorescence signal changed in response to the CS or US, we used a cumulative summation (CuSum) method of detection relative to baseline (Davey et al. 1986). On the first day of conditioning, changes in calcium signals were observed to coincide with US delivery in ~16% of dopamine neurons (24 out of 153 cells; $n = 8$ mice; Fig. 3I) as revealed by a significant deviation of the CuSum (Fig. 3I, inset). This signal was significantly greater than the calcium signal detected during

the corresponding CS− trials (Fig. 3I; two-way repeated-measures ANOVA, $F_{(232,10,904)} = 1.9$, $P < 0.0001$). We did not detect any cells that responded to the CS+. No responses during unpaired CS stimulus presentation or the time corresponding to CS termination were observed in mice that received an unpaired CS (Fig. 3K; $n = 55$ cells; $n = 5$ mice).

On the second day of conditioning, the probe was re-inserted into the VTA and lowered to the same depth as on Day 1. We identified 67 cells in six of eight mice imaged on the second day. Responses to the US were detected in 20% of dopamine neurons (16 out of 67 cells) (Fig. 3J; two-way repeated-measures ANOVA, $F_{(232,6524)} = 2.22$, $P < 0.0001$). Unlike Day 1, on Day 2, CuSum analysis (Fig 3J, inset) revealed changes in calcium signals in 18% of cells in response to CS+ (12 out of 67 cells; Fig. 3D,J). A total of four cells that responded to the US did not respond to the CS and a total of two cells that responded to the CS did not respond to the US.

To compare changes in fluorescence signal associated with US and CS+ presentation in neurons that responded to the US, fluorescence decay was corrected by fitting a curve to each cell during CS− trials and subtracting the fitted curve from the fluorescence during CS+ and CS− trials (Fig. 3M–P). No cells were detected that responded to CS− presentation. Consistent with our CuSum analysis of cells on Day 1 of conditioning, we did not detect significant differences in CS+ trials relative to CS− trials during cue presentation (Fig. 3M); however, changes in fluorescence during US presentation where significantly higher relative to the corresponding time in CS− trials (Fig. 3N; two-way repeated-measures ANOVA, $F_{(84,3948)} = 3.17$, $P < 0.0001$). In cells that responded on the second day of conditioning, both CS+ and US-evoked signals were significantly greater in CS+ trials than CS− trials (Fig. 3O; two-way repeated-measures ANOVA, $F_{(89,2492)} = 2.28$, $P < 0.0001$) (Fig. 3P; two-way repeated-measures ANOVA, $F_{(89,2492)} = 2.73$, $P < 0.0001$).

The nature of behaviorally evoked calcium signals in dopamine neurons has not been previously described. We find that the dynamics of these signals in vivo are similar to those observed during spike firing in vitro, consistent with the activation of dopamine neurons during fear conditioning. The plasticity we observed in calcium signals with conditioning is consistent with the observation of a painful stimulus eliciting synaptic plasticity in discrete populations of VTA dopamine neurons (Lammel et al. 2011). The source of calcium observed during fear conditioning and the contribution of this signal to synaptic plasticity is yet to be resolved. It is intriguing to speculate a potential role for the NMDA-type glutamate receptor, a calcium permeable ion channel critical for both phasic activation of dopamine neurons (Overton and Clark 1997) and synaptic plasticity (Bonci and Malenka 1999). Whether phasic activation of dopamine neurons and plasticity are linked during behavioral conditioning is also an important question that remains to be resolved.

During fear conditioning, we initially observed only responses to the US; however, with additional conditioning, responses to both the US and CS could be observed. Behaviorally, animals tethered to the fiber optic were relatively immobile and their mobility decreased further in both paired and unpaired trials on the second day of conditioning. We did observe significant increases in mobility following foot shock on both the first and second day of conditioning. We also observed significant increases in mobility on the second day in response to the CS+ presentation, relative to CS− presentation and the ITI. This is consistent with mice engaging avoidance behavior and with our observed increase in dopamine signals relating to aversive motivation (Salamone 1994; Badrinarayan et al. 2012).

Numerous studies have investigated the responding of putative dopamine neurons to a variety of conditioned and unconditioned aversive stimuli. These have been performed in anesthetized (Chiodo et al. 1979; Schultz and Romo 1987; Mantz et al. 1989; Ungless et al. 2004; Brischoux et al. 2009) and awake (Mirenowicz and Schultz 1996; Guarraci and Kapp 1999; Joshua et al. 2008; Matsumoto and Hikosaka 2009; Wang and Tsien 2011; Zweifel et al. 2011; Cohen et al. 2012) electrophysiological preparations, along with direct measurements of transient dopamine release (Roitman et al. 2008; Badrinarayan et al. 2012), in mice (Wang and Tsien 2011; Zweifel et al. 2011; Cohen et al. 2012), rats (Chiodo et al. 1979; Mantz et al. 1989; Ungless et al. 2004; Roitman et al. 2008; Brischoux et al. 2009; Badrinarayan et al. 2012), rabbits (Guarraci and Kapp 1999), and monkeys (Schultz and Romo 1987; Mirenowicz and Schultz 1996; Joshua et al. 2008; Matsumoto and Hikosaka 2009). Aversive stimuli used in these studies have included bitter tastants (Roitman et al. 2008), air puff (Mirenowicz and Schultz 1996; Joshua et al. 2008; Matsumoto and Hikosaka 2009; Cohen et al. 2012), shock (Guarraci and Kapp 1999; Ungless et al. 2004; Brischoux et al. 2009; Badrinarayan et al. 2012), and pinch (Chiodo et al. 1979; Schultz and Romo 1987; Mantz et al. 1989; Zweifel et al. 2011), either paired (Mirenowicz and Schultz 1996; Joshua et al. 2008; Matsumoto and Hikosaka 2009; Badrinarayan et al. 2012; Cohen et al. 2012) or unpaired (Chiodo et al. 1979; Schultz and Romo 1987; Mantz et al. 1989; Ungless et al. 2004; Roitman et al. 2008; Brischoux et al. 2009; Wang and Tsien 2011; Zweifel et al. 2011) with conditioning stimuli. The results of these studies have been as varied as the experimental designs, fueling controversies over whether dopamine neurons are, or are not, activated by aversive and fear-inducing stimuli (Schultz 2007; Bromberg-Martin et al. 2010; Lammel et al. 2013; Schultz 2013). Our results obtained through direct visual and genetic isolation of dopamine neurons demonstrate that a subpopulation of dopamine neurons is engaged during fear conditioning.

Although we were able to directly image calcium signals in dopamine neurons, FOC microscopy is not without limitations. We observed significant attrition relating to the ability to image the same number of cells across multiple days using FOC microscopy. Moreover, we are unable to confirm that the same neurons imaged on the first day were imaged on the second day. Resolution is limited to 3.3 μm; thus imaging calcium dynamics in individual dendrites or spines is not possible. In addition, the working distance of the fiber optic is zero; thus cells must be in direct contact with the fiber optic for signal to be detected, limiting the number of cells that can be imaged from a field of view. Finally, the scan rate of 12 Hz precludes high resolution of individual spiking events. Nonetheless, by directly imaging genetically isolated dopamine neurons during Pavlovian fear conditioning, we eliminated confounds associated with characterizing these cells based on pharmacological and electrophysiological response parameters, many of which are not unique to dopamine-producing cells (Margolis et al. 2006). As such, we selectively isolated dopamine neuron responses and demonstrate plasticity in calcium dynamics during fear conditioning, establishing a direct link between activity-dependent processes in dopamine neurons and fear conditioning. Future experiments designed to image dopamine neuron responses to multiple stimuli, with varying intensities, and in projections to specific targets will help to further resolve how these cells respond to different psychophysical stimuli.

Acknowledgments

We thank Graham Jones for technical assistance. This work was supported by the US National Institutes of Health grants R01 MH094536 (L.S.Z.) and T32 DA07278-19 (B.B.G. and M.E.S.).

Author contributions: B.B.G., M.E.S., and L.S.Z. designed and performed research, contributed unpublished reagents/analytic tools, analyzed the data, and wrote the paper.

References

Badrinarayan A, Wescott SA, Vander Weele CM, Saunders BT, Couturier BE, Maren S, Aragona BJ. 2012. Aversive stimuli differentially modulate real-time dopamine transmission dynamics within the nucleus accumbens core and shell. *J Neurosci* **32:** 15779–15790.

Bonci A, Malenka RC. 1999. Properties and plasticity of excitatory synapses on dopaminergic and GABAergic cells in the ventral tegmental area. *J Neurosci* **19:** 3723–3730.

Brischoux F, Chakraborty S, Brierley DI, Ungless MA. 2009. Phasic excitation of dopamine neurons in ventral VTA by noxious stimuli. *Proc Natl Acad Sci* **106:** 4894–4899.

Bromberg-Martin ES, Matsumoto M, Hikosaka O. 2010. Dopamine in motivational control: rewarding, aversive, and alerting. *Neuron* **68:** 815–834.

Chiodo LA, Caggiula AR, Antelman SM, Lineberry CG. 1979. Reciprocal influences of activating and immobilizing stimuli on the activity of nigrostriatal dopamine neurons. *Brain Res* **176:** 385–390.

Cohen JY, Haesler S, Vong L, Lowell BB, Uchida N. 2012. Neuron-type-specific signals for reward and punishment in the ventral tegmental area. *Nature* **482:** 85–88.

Davey NJ, Ellaway PH, Stein RB. 1986. Statistical limits for detecting change in the cumulative sum derivative of the peristimulus time histogram. *J Neurosci Methods* **17:** 163–166.

Guarraci FA, Kapp BS. 1999. An electrophysiological characterization of ventral tegmental area dopaminergic neurons during differential Pavlovian fear conditioning in the awake rabbit. *Behav Brain Res* **99:** 169–179.

Joshua M, Adler A, Mitelman R, Vaadia E, Bergman H. 2008. Midbrain dopaminergic neurons and striatal cholinergic interneurons encode the difference between reward and aversive events at different epochs of probabilistic classical conditioning trials. *J Neurosci* **28:** 11673–11684.

Kerr JN, Nimmerjahn A. 2012. Functional imaging in freely moving animals. *Curr Opin Neurobiol* **22:** 45–53.

Laemmel E, Genet M, Le Goualher G, Perchant A, Le Gargasson JF, Vicaut E. 2004. Fibered confocal fluorescence microscopy (Cell-viZio) facilitates extended imaging in the field of microcirculation. A comparison with intravital microscopy. *J Vasc Res* **41:** 400–411.

Lammel S, Ion DI, Roeper J, Malenka RC. 2011. Projection-specific modulation of dopamine neuron synapses by aversive and rewarding stimuli. *Neuron* **70:** 855–862.

Lammel S, Lim BK, Malenka RC. 2013. Reward and aversion in a heterogeneous midbrain dopamine system. *Neuropharmacology* **79** (Pt B)**:** 351–359.

Mantz J, Thierry AM, Glowinski J. 1989. Effect of noxious tail pinch on the discharge rate of mesocortical and mesolimbic dopamine neurons: selective activation of the mesocortical system. *Brain Res* **476:** 377–381.

Margolis EB, Lock H, Hjelmstad GO, Fields HL. 2006. The ventral tegmental area revisited: Is there an electrophysiological marker for dopaminergic neurons? *J Physiol* **577:** 907–924.

Matsumoto M, Hikosaka O. 2009. Two types of dopamine neuron distinctly convey positive and negative motivational signals. *Nature* **459:** 837–841.

Mirenowicz J, Schultz W. 1996. Preferential activation of midbrain dopamine neurons by appetitive rather than aversive stimuli. *Nature* **379:** 449–451.

Overton PG, Clark D. 1997. Burst firing in midbrain dopaminergic neurons. *Brain Res Brain Res Rev* **25:** 312–334.

Pezze MA, Feldon J. 2004. Mesolimbic dopaminergic pathways in fear conditioning. *Prog Neurobiol* **74:** 301–320.

Roitman MF, Wheeler RA, Wightman RM, Carelli RM. 2008. Real-time chemical responses in the nucleus accumbens differentiate rewarding and aversive stimuli. *Nat Neurosci* **11:** 1376–1377.

Salamone JD. 1994. The involvement of nucleus accumbens dopamine in appetitive and aversive motivation. *Behav Brain Res* **18:** 117–133.

Schultz W. 2007. Multiple dopamine functions at different time courses. *Annu Rev Neurosci* **30:** 259–288.

Schultz W. 2013. Updating dopamine reward signals. *Curr Opin Neurobiol* **23:** 229–238.

Schultz W, Romo R. 1987. Responses of nigrostriatal dopamine neurons to high-intensity somatosensory stimulation in the anesthetized monkey. *J Neurophysiol* **57:** 201–217.

Tian L, Hires SA, Mao T, Huber D, Chiappe ME, Chalasani SH, Petreanu L, Akerboom J, McKinney SA, Schreiter ER, et al. 2009. Imaging neural activity in worms, flies and mice with improved GCaMP calcium indicators. *Nat Methods* **6:** 875–881.

Tian L, Akerboom J, Schreiter ER, Looger LL. 2012. Neural activity imaging with genetically encoded calcium indicators. *Prog Brain Res* **196:** 79–94.

Ungless MA, Grace AA. 2012. Are you or aren't you? Challenges associated with physiologically identifying dopamine neurons. *Trends Neurosci* **35:** 422–430.

Ungless MA, Magill PJ, Bolam JP. 2004. Uniform inhibition of dopamine neurons in the ventral tegmental area by aversive stimuli. *Science* **303:** 2040–2042.

Vincent P, Maskos U, Charvet I, Bourgeais L, Stoppini L, Leresche N, Changeux JP, Lambert R, Meda P, Paupardin-Tritsch D. 2006. Live imaging of neural structure and function by fibred fluorescence microscopy. *EMBO Rep* **7:** 1154–1161.

Wang DV, Tsien JZ. 2011. Convergent processing of both positive and negative motivational signals by the VTA dopamine neuronal populations. *PLoS One* **6:** e17047.

Zhuang X, Masson J, Gingrich JA, Rayport S, Hen R. 2005. Targeted gene expression in dopamine and serotonin neurons of the mouse brain. *J Neurosci Methods* **143:** 27–32.

Zweifel LS, Fadok JP, Argilli E, Garelick MG, Jones GL, Dickerson TM, Allen JM, Mizumori SJ, Bonci A, Palmiter RD. 2011. Activation of dopamine neurons is critical for aversive conditioning and prevention of generalized anxiety. *Nat Neurosci* **14:** 620–626.

Received June 10, 2014; accepted in revised form July 10, 2014.